Plasma enhanced inkjet printing of particle-free silver ink on polyester fabric for electronic devices

Jones, Thomas; Hourd, Andrew; Liu, Tang Chung ; Jia, Lu-Chiang; Lung, Chia-Mei ; Zolotovskaya, Svetlana A.

Published in:
Micro and Nano Engineering

DOI:
10.1016/j.mne.2021.100103

Publication date:
2022

MNE 14 (2022) 100103

Contents lists available at ScienceDirect

Micro and Nano Engineering

journal homepage: www.sciencedirect.com/journal/micro-and-nano-engineering

Research paper

Plasma enhanced inkjet printing of particle-free silver ink on polyester fabric for electronic devices

Thomas D.A. Jones [a,*], Andrew C. Hourd [a], Tang Chung Liu [c], Lu-Chiang Jia [b], Chia-Mei Lung [b], Svetlana Zolotovskaya [a], Amin Abdolvand [a], Chao-Yi Tai [c,*]

[a] Materials Science & Engineering Research Cluster, School of Science and Engineering, University of Dundee, Dundee DD1 4NH, UK
[b] Sousveillance Technology Ltd., Taoyuan 32062, Taiwan
[c] Department of Optics and Photonics, National Central University, 300, Jhongda Road, Jhongli, Taoyuan 32001, Taiwan

ARTICLE INFO

Keywords:
Inkjet
Silver
Particle free
Conductive
Fabric
Polyester
Ink

ABSTRACT

Most formulations of metal inks comprise of a suspension of nanoparticles however, these suffer when printed by the formation of unwanted agglomeration. The exploration and optimisation of particle-free silver-complex ink is causing a strong demand for inkjet printing of these formulations over nanoparticle-based suspension inks. This is due to the enhanced printability and rapid conversion via thermal reduction into a conductive material, which can be utilised in electronics manufacture. We developed a silver-complex ink for 'smart-clothing' through inkjet printing. The high-quality printing - characterised by no satellite droplet formation and fast speed - is demonstrated upon polyester fabric by the formation of electrical circuitry using a thermal reduction process. Fabric printing is limited by good metal coverage and adhesion, which we demonstrate and improve on in the work by the application of a low temperature, atmospheric air plasma pre-treatment to the polyester surface, which improves printed silver density and coverage using a plasma device which is easy to operate and economic. Printed silver layer reduction and film crystallinity is characterised from high resolution scanning electron microscopy, and spectroscopy (Ultraviolet-visible and Raman) detailing growth mechanisms for high track feature conductivity, producing a low sheet resistivity of $1.378 \pm 0.001\ \Omega/\square$ and by the lighting of a 1.9 V, 250 mA Light Emitting Device, highlighting its application for conductive features processing.

1. Introduction

Within the last decade considerable developments have occurred in the fabrication of wearable electronics. This includes electromechanical devices such as sensors for activity monitoring, memory devices, portable displays and self-powered devices [1]. Polyester or polyethylene terephthalate (PET) is an economic, versatile fabric applied extensively in clothing. Its properties enable chemical treatment of metal ions into its surface, to produce high strength conductive electronic features [2]. PET has high melting/glass transition (dependent on it having semicrystalline or amorphous structures, respectively) and combustion temperatures relative to nylon or polycarbonate, indicating that it is a good material of choice to survive the thermal processing conditions used in micro-track feature fabrication [3] and for the development of wearable electronics.

The existing methods for fabric microelectronic fabrication techniques include photolithography [4], electroless plating processes [5,6] and vacuum deposition [7] show disadvantages such as high cost of equipment, multistage processing requirements and a large degree of environmental waste. Alternative, economical printing techniques include screen printing, roll-to-roll printing, gravure printing, flexographic printing and inkjet printing [8]. Inkjet printing is becoming a widely established method for the manufacture of electrical devices, due to the low equipment costs and wide range of printable metallic inks [1,2].

Popular formulations of metal inks comprise of a suspension of nanoparticles however, these suffer when printed by the formation of unwanted agglomeration, which can contribute to nozzle blocking, a reduction in printed feature resolution [9] and poor uniformity from 'coffee-stain' effect [10]. Particle free inks are an alternative formulations addressing all of these issues, whose examples include organometallic platinum (Pt) [9] and silver (Ag) [8], which have been printed with lower processing temperature requirements compared to their agglomerated-ink alternatives. As such, particle-free inks are highly

* Corresponding authors.
E-mail address: t.d.a.jones@dundee.ac.uk (T.D.A. Jones).

https://doi.org/10.1016/j.mne.2021.100103
Received 30 August 2021; Received in revised form 14 December 2021; Accepted 26 December 2021
Available online 29 December 2021

suitable for large-scale manufacturing processes due to their increased printability, high versatility, and quality.

Recently, a novel particle-free formulation for the formation of Ag ink for screen printing has been introduced by the authors [11], which comprises of a stable silver complex formed from the addition of ammonium carbonate to silver oxide [12]. Silver complexes are ideal substitutes to particle dispersions for the formation of conductive features on textiles [13]. Here, we present the evaluation of ink print properties for inkjet printing applications for fabric. The formation of Ag metal features from printed ink is possible by reduction, which can be achieved either chemically, optically, by high energy radiation, or thermally [4,7]. Thermal reduction is particularly suitable to Ag particle-free inks due to the relatively low temperatures, 180 °C and fast processing times (10 min) [3,14].

The choice of PET fabric thicknesses differs dependent on their application and use. When printing onto PET fabrics of different density ink spreading varies dependent on the weave pattern, thread size and thickness of the PET substrate [15] and so, two PET samples of differing size were evaluated within this study to determine the printability on each.

To improve the Ag metal reduction and printed quality, pre-treatment of the substrates either chemically [7], acoustically or optically [16] can be applied. Plasma treatment of PET has been shown to increase its surface energy and wettability leading to increased Ag uptake, however this can require low pressures and selective gasses, (oxygen, argon and helium) [17]. An economic, more environmentally friendly and accessible pre-treatment is the use of low temperature, atmospheric pressure air plasma [18], which can provide enhancements for silver deposition onto PET [19]. Atmospheric plasma offers additionally a more economic, portable less cumbersome setup where a vacuum chamber or a gas flow is not required. Air plasma has also been shown to be more efficient at wetting PET than oxygen-containing argon or helium plasma treatments, due to the more rapid reactions occurring between the oxygen species and the created radicals on the surface [17]. For these reasons, an investigation was performed looking to improve the wettability of the reduced particle-free Ag printed ink using an atmospheric air plasma treatment of the PET fabrics.

In this work the printability of the Ag particle-free ink was assessed from evaluations of its surface tension and contact angle, using pendant drop equipment, which highlighted the printability of the ink - its Z number [20] - and optimisation of the plasma corona treatments from evaluations of fabric surface energy, which led to evaluations of optimum printer driving conditions. The evaluation of thermally reduced printed Ag quality and crystallinity on different thickness PET samples was conducted using electron and optical microscopes, and spectroscopic techniques (Ultraviolet-visible (UV–vis), Raman); and deposit composition and uniformity by Energy Dispersive X-ray (EDX). The deposit adhesive and electrical properties due to the application of plasma treatment were evaluated using the so-called “Scotch tape” test [16], four-point probe measurements and the demonstration of the lighting of a light emitting device (LED) using the printed features.

2. Experimental

For complete details of experimental see supplemental information.

2.1. Ag ink formulation, testing and jetting

The particle free Ag-based ink was formulated as described previously [11], which comprises of a stable silver complex formed from the addition of ammonium carbonate to silver oxide along with ethylmethylamine and ethylene glycol [12]. The dynamic viscosity (η) of the ink was evaluated using a Cannon-Fenske Viscometer, at 25 °C as 12 ± 0.5 *m*Pa.s. The *Z*-number for the ink was evaluated using:

$$Z = \frac{(a\rho\gamma)^{0.5}}{\eta} \quad (1)$$

Where a is the diameter of the drop-on-demand printer nozzle (21.5 μm); ρ is the density of the ink (1141.5 kg/m^3); and γ is the surface tension of the ink (26.96 ± 0.15 *m*N/m) evaluated using the Kruss EasyDrop™ software [9].

The contact angle was measured using the Kruss EasyDrop™ and the surface energy evaluated using the Wu method [21] using contact angles obtained from DI water and diiodomethane.

2.2. Ink printing onto PET

Two 100% PET fabric samples of thicknesses 0.75 ± 0.05 mm (110 g/m^2), and 0.07 ± 0.01 mm (41 g/m^2) were printed onto using a Fuji-Film Dimatix DMP-2831 [10]. For print details see supplemental section A2, fig. A1.

An atmospheric air plasma treatment was applied to the PET using a 5–30 W, 230 V BD-20 AC 50/60 Hz (electro-technic) Laboratory Corona Treater for treatment times between 30 and 1800 s. The plasma treatment power (TP) was estimated at between 7 and 400 kJ/m^2, from:

$$TP = \frac{nP}{lv} \quad (2)$$

where n is the number of passes (equivalent to the treatment time), P is the output power (~ 15 W), l is the electrode length (6.75 cm) and v is the average velocity of the electrode across the fabric surface (~ 1 m/s) [22] .

2.3. Print characterisation

Effect of the plasma treatment on the Raman response of the PET fabric samples were examined using an in-house built Raman microprobe system.

For testing adhesion and quantifying thermal reduction, 5 cm^2 PET samples were dipped into a solution of the Ag ink and thermally reduced in an oven for 10 min at 180 °C from settings chosen from within [4,14]. Reduced-Ag feature adhesion to the PET was tested using the so-called ‘Scotch tape’ method on the 0.75 mm sample (0.07 mm unsuitable for testing) and afterwards, the tape samples were then placed onto white paper for inspection where optical images were obtained and contrast enhancement performed using ImageJ. Sample wash performance was investigated on both fabrics by testing within an Ultrasonic bath (Jenscon) with a DI water rise for 30 min after Ag thermal reduction onto PET. The bending and stretching electrical performance was also tested. Thermal reduction was quantified on PET samples using a UV–Vis spectrophotometer (Jasco, V600) operating in absorption mode.

After printing, the samples were thermally reduced at 180 °C and printed features evaluated from the electrical sheet resistivity using a (Ossila) four-point probe station. To demonstrate the electrical conductivity of the printed Ag, the lighting of a 1.9 V, 250 *m*A green Light Emitting Diode (LED) (supplied from RS) was demonstrated by constructing a series circuit with a 9 V battery and a 1.5 kΩ, 250 *m*W resistor.

Cross sections of the printed fabric were obtained by cutting the fabric with a knife. High resolution images of the surface were obtained using an optical microscope (Spectrographic, NMM-800RF) and a Field Emission Scanning Electron Microscope (SEM) (JSM-7400F, JEOL). EDX analysis was performed on the printed surface using the SEM equipment.

3. Results and analysis

3.1. Evaluated ink printing characteristics

Before printing the properties of the ink were evaluated from

measurements of a droplet of ink of area 10 ± 0.5 mm^2 suspended from a syringe including its surface tension, as see Fig. 1A. The surface tension of the fluid was evaluated as 26.7 ± 0.3 *m*N/m. This value indicates that the ink is suitable for rapid jetting as values beyond 25 *m*N/m show good printing properties for rapid printing [9].

The viscosity and density of the ink was measured as 12 *m*Pa.s and 1.1415 g/mL, respectively and using these values the Z number of the ink was evaluated as 2.14, which is within an acceptable range for inkjet printing (1−10) [20].

The printing voltage waveform settings for the ink were optimised from observations of the jetting of the ink within the Dimatix printer head. Highlighted in Fig. 1B, is an optical image taken from a high-speed camera within the Dimatix printer setup, of three 10 pL ink droplets shown as the dark dots by the blue arrow. They have been ejected downwards and a stationary image captured with a 100 μs refresh rate. Using this knowledge and the position of the droplets relative to the nozzle (800 μm), a drop velocity of 8 m/s was evaluated. Values of 1 to 20 m/s are regarded as acceptable, as values lower than this produce poorer drop positioning or provide insufficient kinetic energy for the droplet to escape the nozzle; and higher values induce non-uniform splashing upon substrate. The measured value is within this range indicating a good velocity. A high droplet quality was identified as displayed in the supplemental section B, along with the determined optimal voltage waveform setting.

3.2. Ag inkjet printing onto PET

Particle-free Ag ink printing was characterised on the 0.75 mm, 110 g/m^2 PET fabric with the printed results displayed in Fig. 2. Shown in A and B is the surface after twelve layers printing for before and after thermal reduction, respectively. Thermal reduction changes the appearance of the surface from a dark colour to a lighter shade, which corresponds to the modification of the Ag^+ ions to the Ag^0 metal via the thermal reduction process [23].

Highlighted in Fig. 2C is a top-down SEM image of the thermally reduced PET surface with Ag metal. The image displays the edge of the track feature showing divided by the dashed line, non-printed and printed regions at top and bottom, respectively. The Ag pattern forms on the PET fibres as a matt deposit. A well-defined interface between the printed and non-printed regions is observed which indicates good feature resolution after printing. EDX scans of the surfaces reveal that the printed and non-printed regions contain 68 wt% and 0 wt% Ag, respectively, highlighting further the fine feature definition. Other elements detected were C, O and Al. The C and O were present within the PET fibre and the Al is likely the metal base of the SEM sample holder.

The penetration of the printed ink into the fabric was characterised in Fig. 2D, from cross-section analysis of the fabric under SEM/EDX. The top of the image shows the region where the fabric was printed onto. From the top of the fabric to the backside where it was not printed, EDX was obtained over five-regions, highlighted in D, each covering an area of approximately 0.225 mm^2. The elemental distribution for the different regions was plotted in Fig. 2E, showing the Ag composition reduce from 47 wt% at the top printed side to 27 wt% at the backside. This indicates that for the twelve printed layers the Ag ink had absorbed through the PET and formed metal deposit throughout, however with a thinner deposit toward the back side.

Thermal reduction process was captured from the PET for treatment with Ag, before and after thermal reduction, see supplemental section C, highlighting peaks characteristic of Ag nanofilms after reduction.

3.3. Improvements to print wettability and electrical durability

The 0.75 mm, 110 g/m^2 PET fabric was treated with a plasma torch of powers 0 kJ/m^2, 27 kJ/m^2, 67 kJ/m^2, 130 kJ/m^2 and 400 kJ/m^2, to alter its surface. Highlighted in Fig. 3A and B are SEM images of its before and after treatments, respectively. Without the plasma torch the individual threads of the PET surface can be seen within the weave. The plasma torch was applied for 27 kJ/m^2 exposure and showed little change in the outward appearance of the PET threads, as observed in [24] for similar treatments. For a prolonged exposure of 400 kJ/m^2 to exaggerate its influence, the PET fabric thread structure can no longer be seen, replaced by a melted surface structure which has also been reported for highly localised plasma discharging onto PET [25]. The changes to PET surface morphology expected include surface roughness increases [24] and structure oxidation of the PET surface breaking ester bonds and forming radicals which react with the plasma gas generated to form hydroxyl, carbonyl, and carboxyl groups, see supplemental Fig. A1.

The adhesion of Ag deposited onto the PET by dipping was evaluated as shown by the tape test results of the 0.75 mm sample (Fig. 3C). Contrast enhanced optical images of the tape produced after the testing is displayed showing in dark Ag deposit removed after test. For increasing treatments 0 kJ/m^2, 27 kJ/m^2 and 67 kJ/m^2, the amount of Ag removed successively reduced indicated by the lighter shade of the image, showing potential improvements to adhesion of the deposit with the PET. This highlights that owing to greater ink penetration by the application of plasma, the Ag removal was reduced as typical losses of silver occur on fabric surfaces [26].

The sheet resistivity was measured on the samples after tape testing indicating that conductivity could still be obtained and that it increased by approximately a factor of 10 (2.28 to 21.1 Ω/□) for the increasing plasma treatments, which was likely due to an increased fabric roughness induced by the plasma [27], resulting in an increase to the numbers of scattering centres for the conduction electrons.

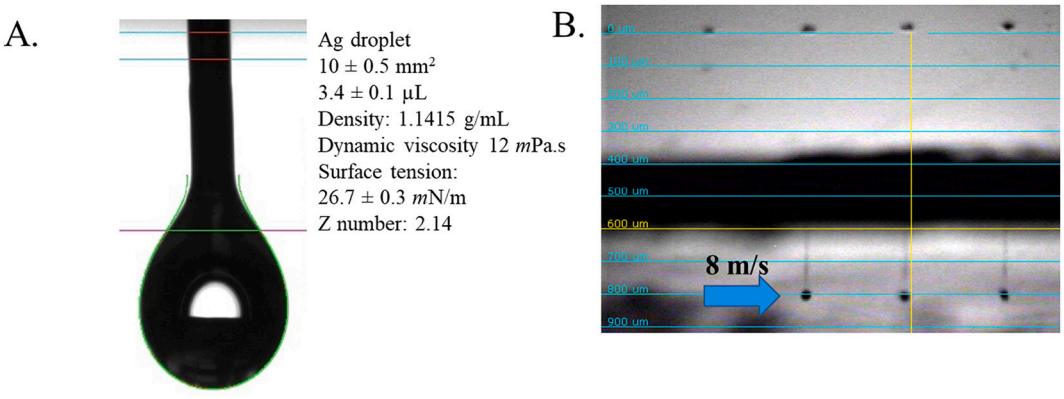

Fig. 1. A) Pendant Drop testing of the ink. B) Optical image of the jetting of three 10 pL, 8 m/s, ink droplets (blue arrow) by high speed camera within Dimatix printer. (For interpretation of the references to colour in this figure legend, the reader is referred to the web version of this article.)

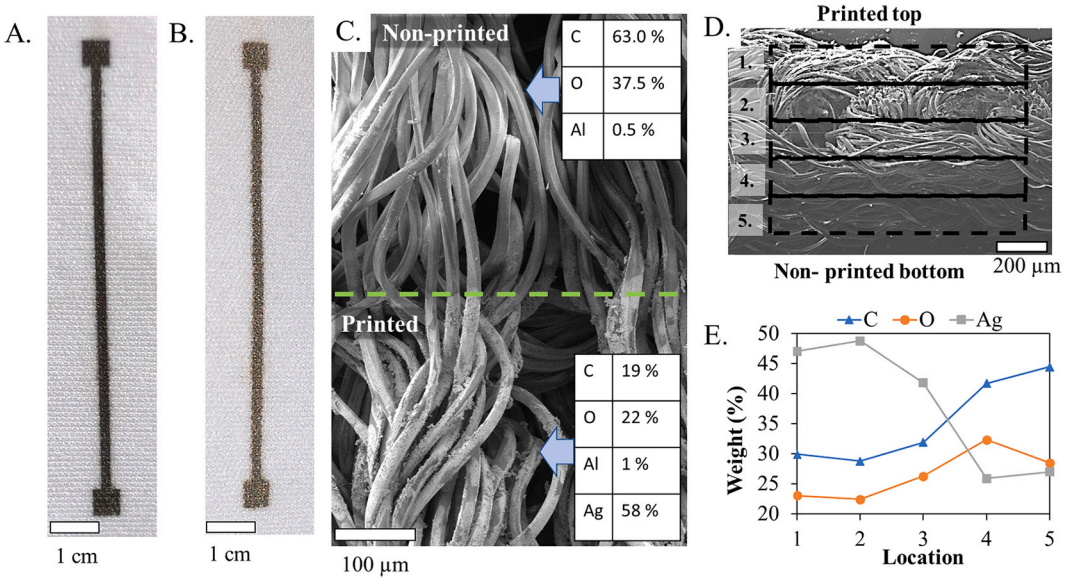

Fig. 2. Twelve-layer Ag inkjet printed 0.75 mm thick, 110 g/m^2 PET surface, non-plasma treated. A) and B), optical images before and after thermal reduction for 10 min at 180 °C, respectively. SEM images showing C) top-down view, and D) cross-sectional views of printed surface. E) plot of EDX elemental wt% composition across the cross section of the fabric for locations highlighted in D).

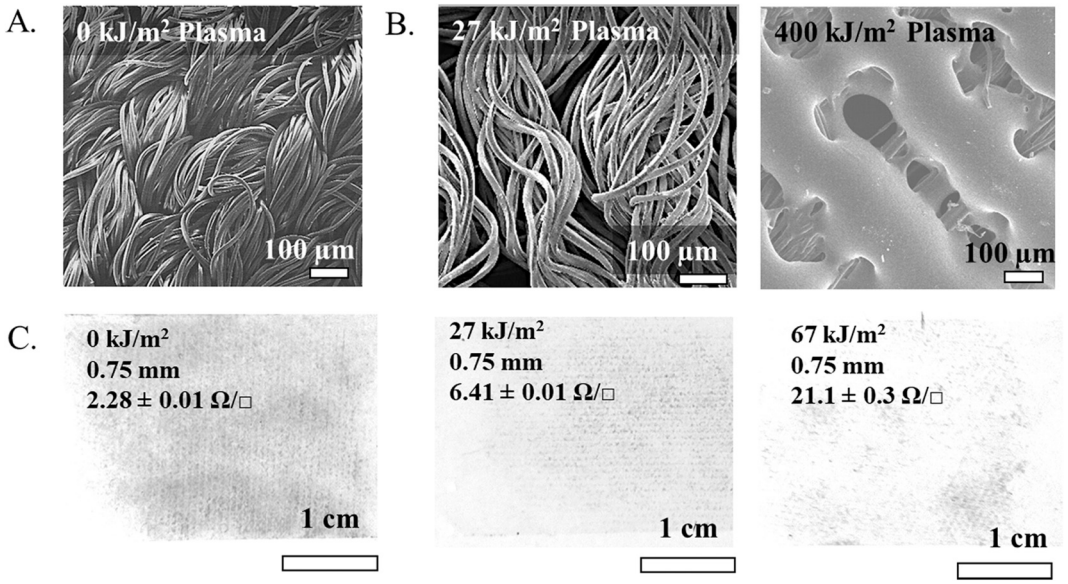

Fig. 3. Atmospheric Plasma treatment of 0.75 mm, 110 g/m^2, PET fabric. A) & B) SEM images of none and with exposures, respectively. C) Tape test adhesion results of applied and reduced Ag on plasma treated and non-treated 0.75 mm, 110 g/m^2 surfaces. Contrast enhanced images.

The influence of plasma on the PET was analysed from Raman scans of the 0.07 mm, 41 g/m^2 fabric, see supplemental section D, and changes to the PET surface chemistry were observed induced by the plasma treatment.

A good conductivity stability was indicated from successive tape tests applied to a 24-layer printed 0.75 mm thick sample, with 27 kJ/m^2 and 0 kJ/m^2 treatments (see supplemental section E). The wash performance was also conducted on both PET thicknesses dip-treated with Ag, and with/without plasma treatments (see supplemental section E) to display a good electrical durability after washing.

The bending and stretching performance were tested, see supplemental section H. The results show good bending performance and stretching up to 20% strain. For applications relating to flexible sensors on clothing this indicates increased longevity of the print feature conductivity.

The optimal plasma treatments required for wetting of the two PET samples were evaluated see supplemental section F, highlighting that for TP of 27 kJ/m^2 no further improvements to wetting were obtained.

The Ag formation was quantified on the 0.07 mm thick sample using six layers of Ag printing and TP of 27 kJ/m^2. Highlighted in Fig. 4 are SEM images of the thermally reduced surfaces showing top-down images of the printed surfaces. For the non-plasma treated surface (Fig. 4A), the deposit is looser and flakier than its plasma treated equivalent (Fig. 4C). The samples were both conductive showing similar sheet resistivities of 1.26 ± 0.07 Ω/□ and 1.22 ± 0.42 Ω/□, accordingly. On closer inspection of the deposit, without plasma an SEM image (Fig. 4B) taken from a region where the Ag deposit was not flaky, shows a uniform, polycrystalline isotropic Ag deposit whereas, for the plasma treated PET (Fig. 4D) Ag rich (57%) hexagonal, anisotropic crystals of sizes ranging from 0.7–1.3 µm are observed. Ag hexagonal crystalline phase can form

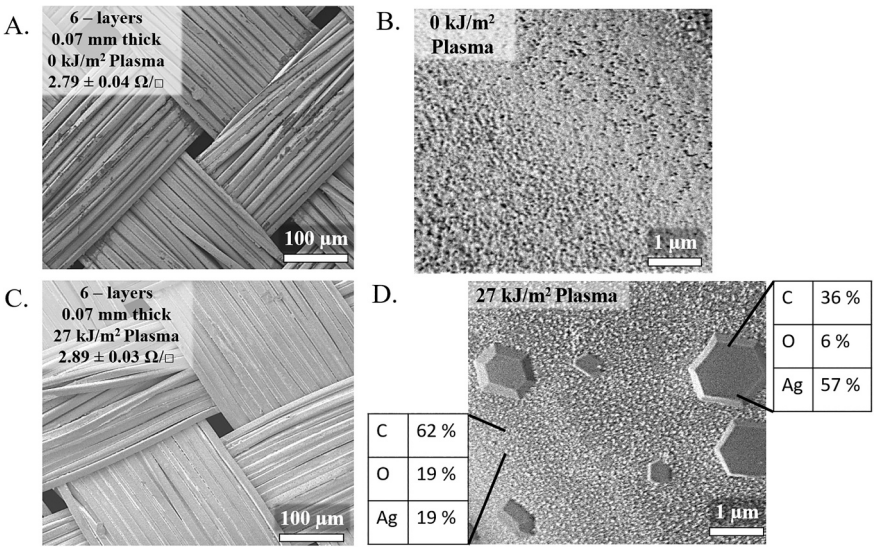

Fig. 4. SEM image of 0.07 mm thick PET after six layers Ag printed and thermal reduction for A) & B) no plasma and C)&D) with 2 min plasma. Inserts, EDX elemental data.

[28], and their formation as nanoplatelets has been attributed to the combination or growth via Ostwald ripening of smaller less thermodynamically stable triangular Ag nanoplatelets [29]. Their here is likely a combination of inhomogeneous growth conditions, induced by the corona stream due to electrical grounding between the PET threads, as witnessed in [25]. This effect would be more prevalent on the thinner

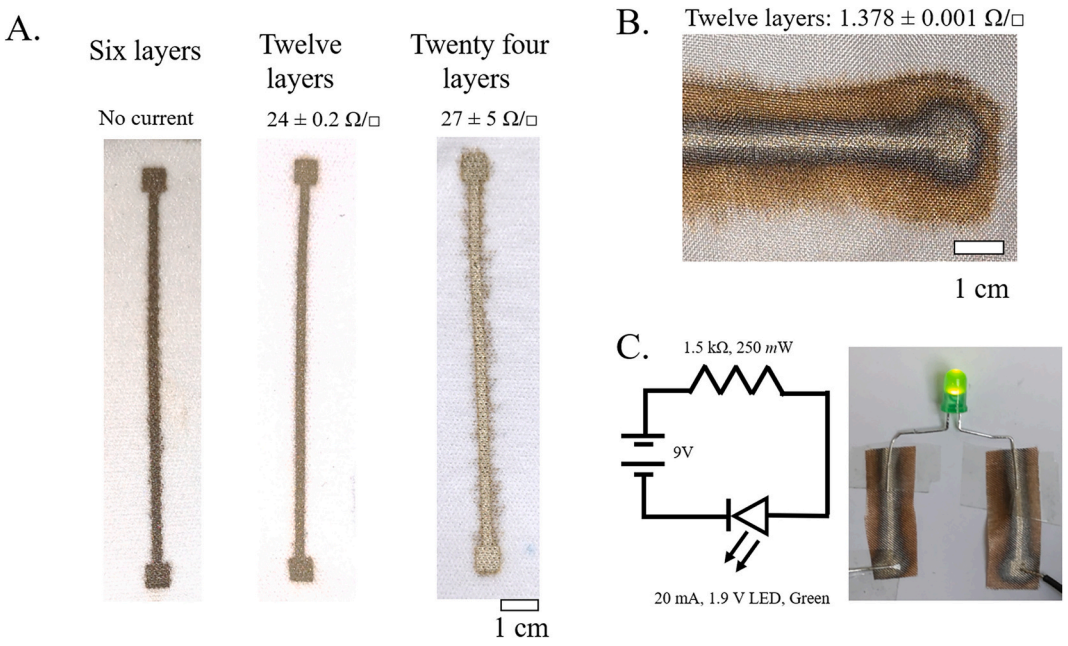

D.

Numbers of printed layers	Sheet resistance (Ω/□) 0.75 mm		0.07 mm	
	0 kJ/m²	27 kJ/m²	0 kJ/m²	27 kJ/m²
4	Unable to measure	256 ± 5	-	-
6	Unable to measure	-	2.79 ± 0.04	2.89 ± 0.03
12	24 ± 0.2	-	1.378 ± 0.001	-
24	27 ± 5	24 ± 3	-	-

Fig. 5. Electrical resistivity of printed and thermally reduced Ag on non-plasma treated A) 0.75 mm thick PET for increased printed layers and B) twelve layers, 0.07 mm thick PET. C) Demonstration of lighting of 1.9 V, 250 mA, LED from twelve layer printed, 0 kJ/m^2, 0.07 mm thick fabric. D) summary of sheet resistivity measurements.

less dense 0.07 mm sample due to an increased likelihood of electrical grounding, which is a possible reason why the hexagonal deposit formation was not observed on the thicker 0.75 mm sample, see supplemental section G.

Surrounding the hexagonal deposits is an Ag deposit of lower concentration (19 wt%) which is nodular, uniform and more randomly oriented. The texturing of the PET surface is also different compared to the non-plasma condition (Fig. 4C). Plasma treatment can increase surface roughness of PET fabric [27] and so the texturing of the plasma treated surface here is likely influenced by this.

SEM scans of the 0.75 mm thick PET with TP 27 kJ/m^2 and four layers of Ag were shown within supplemental section G. Here the sheet resistance was lower owing to its lower wettability (see section F, supplemental) and larger number of printed layers. Unlike the thinner material it was not possible to obtain an electrical measurement without the application of the plasma.

The printed performance was further investigated on non-plasma treated PET surfaces to highlight the relationship of print layers on sheet resistivity. Highlighted in Fig. 5A are images of 0.75 mm thick PET surface after Ag printing of six, twelve and twenty-four layers with thermal reduction. The surfaces show qualitatively a change in appearance with a lighter colour on the application of greater layers along with a loss of feature definition, corresponding to an increased uptake of silver and spreading (see supplemental section F). The spreading was additionally due to a misalignment of droplet placement onto the PET caused by droplet build-up on the dimatix cartridge head which had dried with prolonged use, deflecting the ejected droplets from the cartridge head nozzles. Further optimisation of printer cleaning cycles could improve on this unwanted effect. The sheet resistivity was measured across the twelve layer and twenty-four-layer printed samples as 24.0 ± 0.2 Ω/□ and 27 ± 5 Ω/□, respectively, indicating that for increased printed layers beyond twelve no further reduction of resistivity was measured. For the six-layer printed sample, it was not possible to measure the resistivity as no current could be drawn. This was likely due to the Ag being too thin as shown when printing four layers onto 0.75 mm (see supplemental section G).

Twelve layers of Ag-lines were inkjet printing on top of a thinner (0.07 mm) PET sample and thermally reduced, as shown in Fig. 5B. Spreading of the ink had occurred across the PET surface highlighted by a dark-brown periphery around the printed track. The increased surface energy of the thinner sample (see supplemental section F) meant that increased spreading occurred across the fibre surface and a lower defined feature resolution was obtained than for the 0.75 mm thick PET. However, the electrical sheet resistivity of the printed features on the 0.07 mm substrate was significantly lower than the 0.75 mm substrate for twelve printed layers, 1.378 Ω/□ verses 24.0 ± 0.2 Ω/□, respectively. This was likely due to the thinner fabric showing increased wettability and smaller thickness, and so a greater percentage of its internal structure absorbing the ink to produce a more uniform conductive feature after thermal reduction.

To demonstrate the conductivity of the twelve-layer printed 0.07 mm thick substrate, a 9 V, 20 *m*A LED was lit by placing the printed features within a series circuit with the LED, see Fig. 5C using track feature from 5B. The successful lighting indicates that the printed tracks have a sufficient conductivity to light an LED regardless of whether plasma treatment was applied, although the numbers of printed layers required to achieve conductivity is higher. A table summarising the different samples printed and their numbers of layers is highlighted in Fig. 5D showing reduced electrical sheet resistance on application of layers and by increasing the surface energy via plasma and thinner substrate choices. The measured sheet resistances match other reported values for printed particle-free Ag on PET fabric(0.9 ± 0.02 Ω/□ [2], 1.387 ± 0.001 Ω/□ [this work]), also see supplemental section I. With the two fabric samples a trade-off between electrical conductivity and feature resolution is made due to the differing surface energies and print performances.

4. Conclusions

A particle-free, Ag-complex ink's printability was demonstrated for applications to microelectronics fabrication on PET fabric substrates of different thickness and surface treatment. Ink printing quality was demonstrated from measures of its surface tension, which showed suitability for rapid printing, highlighting the ink's applicability to high volume printing applications. Print jetting conditions were determined and demonstrated by the successful printing of the ink onto PET fabric surfaces. Thermal reduction techniques were applied and measured, transforming the printed ink from ionic form to silver features of high feature definition, good adhesion, washability, and low electrical resistivity. Printed Ag film crystallinity was monitored and characterised on different fabric densities, and fabric specific formation mechanisms were highlighted showing localised regions of high density crystallinity. High conductivity was demonstrated by the lighting of an LED utilising inkjet printed tracks into a series circuit, demonstrating its use for 'smart fabric' applications. The printed track conductivity was enhanced by increasing the numbers of printed layers and reducing the PET material density, although the track definition deteriorated for application of these parameters, due to an increased spreading of the ink related to its surface energy. Penetration of the ink into the fabric was monitored and highlighted that the printed ink processed through ensuring greater conductive durability.

Printed ink wettability and adhesion on PET fabrics was enhanced and optimised by the application of atmospheric air plasma surface treatment. An ideal treatment power was determined beyond which no further enhancement to wettability was monitored. The treated surfaces enabled the printing of Ag features showing improved Ag deposit coverage and increased Ag volume for the equivalent number of printed layers without plasma. This enables fewer numbers of printing layer to be applied to the polymer's surface before a conductive surface is achieved. The atmospheric plasma treatment process provides a low-cost rapid pre-treatment method to reduce the numbers of printed layers on the fabrics and is suitable for improving the product lifetime of printed microelectronics into clothing.

Declaration of Competing Interest

The authors declare that they have no known competing financial interests or personal relationships that could have appeared to influence the work reported in this paper.

Acknowledgments

Chao-Yi Tai and Amin Abdolvand acknowledge the British Office Taipei for the funding support by the UK-TW Innovative Industries Researcher Placement Scheme. They thank the Ministry of Science and Technology (MOST, Taiwan) and the Royal Society of Edinburgh for support through the Bilateral Visits Programme (BVP, 108-2911-I-008-508). Chao-Yi Tai is also grateful to the MOST for the support under Add-on Grant for International Cooperation scheme with contract MOST 107-2112-M-008-010. For Raman spectroscopy Svetlana Zolotovskaya and Amin Abdolvand acknowledge support from EPSRC through EP/P008135/2 and EP/S017445/1.

Appendix A. Supplementary data

Supplementary data to this article can be found online at https://doi.org/10.1016/j.mne.2021.100103.

References

[1] M. Gao, L. Li, Y. Song, Inkjet printing wearable electronic devices, J. Mater. Chem. C 5 (2017) 2971–2993, https://doi.org/10.1039/C7TC00038C.

[2] H. Shahariar, I. Kim, H. Soewardiman, J.S. Jur, Inkjet printing of reactive silver ink on textiles, ACS Appl. Mater. Interfaces 11 (2019) 6208–6216, https://doi.org/10.1021/acsami.8b18231.
[3] W.-G. Kwak, J.-R. Cha, M.-S. Gong, Surface modification of polyester fibers by thermal reduction with silver carbamate complexes, Fibers Polym. 17 (2016) 1146–1153, https://doi.org/10.1007/s12221-016-5786-3.
[4] A. Ryspayeva, T.D.A. Jones, M.N. Esfahani, M.P. Shuttleworth, R.A. Harris, R. W. Kay, M.P.Y. Desmulliez, J. Marques-Hueso, Selective electroless copper deposition by using photolithographic polymer/Ag nanocomposite, IEEE Trans. Electron Dev. (2019) 1–6, https://doi.org/10.1109/TED.2019.2897258.
[5] A. Ryspayeva, T.D.A. Jones, S.R. Khan, M.N. Esfahani, M.P. Shuttleworth, R. A. Harris, R.W. Kay, M.P.Y. Desmulliez, J. Marques-Hueso, Selective metallization of 3D printable thermoplastic polyurethanes, IEEE Access (2019) 1, https://doi.org/10.1109/ACCESS.2019.2931594.
[6] T.D.A. Jones, A. Bernassau, D. Flynn, D. Price, M. Beadel, M.P.Y. Desmulliez, Analysis of throwing power for megasonic assisted electrodeposition of copper inside THVs, Ultrasonics (2020), 106111, https://doi.org/10.1016/j.ultras.2020.106111.
[7] T.D.A. Jones, A. Ryspayeva, M.N. Esfahani, M.P. Shuttleworth, R.A. Harris, R. W. Kay, M.P.Y. Desmulliez, J. Marques-Hueso, Direct metallisation of polyetherimide substrates by activation with different metals, Surf. Coat. Technol. 360 (2019) 285–296, https://doi.org/10.1016/j.surfcoat.2019.01.023.
[8] M. Vaseem, G. McKerricher, A. Shamim, Robust design of a particle-free silver-organo-complex ink with high conductivity and inkjet stability for flexible electronics, ACS Appl. Mater. Interfaces 8 (2016) 177–186, https://doi.org/10.1021/acsami.5b08125.
[9] D.M. Goldie, A.C. Hourd, M.R. Harvie, J. Thomson, A. Abdolvand, Scatter-limited conduction in printed platinum nanofilms, J. Mater. Sci. 50 (2015) 1169–1174, https://doi.org/10.1007/s10853-014-8673-6.
[10] A.C. Hourd, R.T. Baker, A. Abdolvand, Structural characterisation of printable noble metal/poly(vinyl-alcohol) nanocomposites for optical applications, Nanoscale 7 (2015) 13537–13546, https://doi.org/10.1039/c5nr03636d.
[11] L.C. Jai, C.M. Lung, Silver Conductive Ink and its Preparation TW I671367 B, TW I671367 B, 2019.
[12] K.-C. Chung, H.-N. Cho, M.-S. Gong, Y.-S. Han, J.-B. Park, D.-H. Nam, S.-Y. Uhm, Young-Kwan Seo, Organic Silver Complexes, their Preparation Methods and their Method for Forming Thin Layers, US 2013/0022761 A1, 2013.
[13] J. Kastner, T. Faury, H.M. Außerhuber, T. Obermüller, H. Leichtfried, M. J. Haslinger, E. Liftinger, J. Innerlohinger, I. Gnatiuk, D. Holzinger, T. Lederer, Silver-based reactive ink for inkjet-printing of conductive lines on textiles, Microelectron. Eng. 176 (2017) 84–88, https://doi.org/10.1016/j.mee.2017.02.004.
[14] K.C. Chung, M.S. Gong, J. Shim, Organic Silver Compound and it's Preparation Method, Organic Silver Ink and it's Direct Writing Method, US 7,618,561 B2, US 7,618,561 B2, 2009.
[15] H. Park, W. Carr, H. Ok, S. Park, Image quality of inkjet printing on polyester fabrics, Text. Res. J. 76 (2006) 720–728, https://doi.org/10.1177/0040517507074368.
[16] J. Marques-Hueso, T.D.A. Jones, D.E. Watson, A. Ryspayeva, M.N. Esfahani, M. P. Shuttleworth, R.A. Harris, R.W. Kay, M.P.Y. Desmulliez, A rapid photopatterning method for selective plating of 2D and 3D microcircuitry on polyetherimide, Adv. Funct. Mater. 28 (2018) 1–8, https://doi.org/10.1002/adfm.201704451.
[17] N. De Geyter, R. Morent, C. Leys, L. Gengembre, E. Payen, Treatment of polymer films with a dielectric barrier discharge in air, helium and argon at medium pressure, Surf. Coat. Technol. 201 (2007) 7066–7075, https://doi.org/10.1016/j.surfcoat.2007.01.008.
[18] K. Haubert, T. Drier, D. Beebe, PDMS bonding by means of a portable, low-cost corona system, Lab Chip 6 (2006) 1548–1549, https://doi.org/10.1039/B610567J.
[19] A. Ryspayeva, T.D.A. Jones, M.N. Esfahani, M.P. Shuttleworth, R.A. Harris, R. W. Kay, M.P.Y. Desmulliez, J. Marques-Hueso, A rapid technique for the direct metallization of PDMS substrates for flexible and stretchable electronics applications, Microelectron. Eng. 209 (2019) 35–40, https://doi.org/10.1016/j.mee.2019.03.001.
[20] A. Soleimani-Gorgani, in: J. Izdebska, S.B.T.-P. on P. Thomas (Eds.), 14 - Inkjet Printing, William Andrew Publishing, 2016, pp. 231–246, https://doi.org/10.1016/B978-0-323-37468-2.00014-2.
[21] S. Wu, Calculation of interfacial tension in polymer systems, J. Polym. Sci. Part C Polym. Symp. 34 (1971) 19–30, https://doi.org/10.1002/polc.5070340105.
[22] F.R. Oliveira, M. Fernandes, N. Carneiro, A. Pedro Souto, Functionalization of wool fabric with phase-change materials microcapsules after plasma surface modification, J. Appl. Polym. Sci. 128 (2013) 2638–2647, https://doi.org/10.1002/app.38325.
[23] W.-G. Kwak, M.H. Oh, S.-Y. Son, M.-S. Gong, Silver loading on poly(ethylene terephthalate) fabrics using silver carbamate via thermal reduction, Macromol. Res. 23 (2015) 509–517, https://doi.org/10.1007/s13233-015-3069-2.
[24] S. Klébert, S. Tilajka, L. Románszki, M. Mohai, E. Csiszár, Z. Károly, Degradation phenomena on atmospheric air plasma treatment of polyester fabrics, Surf. Interface 22 (2021), 100826, https://doi.org/10.1016/j.surfin.2020.100826.
[25] G. Borcia, C.A. Anderson, N.M.D. Brown, Surface treatment of natural and synthetic textiles using a dielectric barrier discharge, Surf. Coat. Technol. 201 (2006) 3074–3081, https://doi.org/10.1016/j.surfcoat.2006.06.021.
[26] A. Bacciarelli-Ulacha, E. Rybicki, E. Matyjas-Zgondek, A. Pawlaczyk, M. I. Szynkowska, A new method of finishing of cotton fabric by in situ synthesis of silver nanoparticles, Ind. Eng. Chem. Res. 53 (2014) 4147–4155, https://doi.org/10.1021/ie4011113.
[27] J. Molina, J. Fernández, M. Fernandes, A.P. Souto, M.F. Esteves, J. Bonastre, F. Cases, Plasma treatment of polyester fabrics to increase the adhesion of reduced graphene oxide, Synth. Met. 202 (2015) 110–122, https://doi.org/10.1016/j.synthmet.2015.01.023.
[28] I. Chakraborty, D. Carvalho, S.N. Shirodkar, S. Lahiri, S. Bhattacharyya, R. Banerjee, U. Waghmare, P. Ayyub, Novel hexagonal polytypes of silver: growth, characterization and first-principles calculations, J. Phys. Condens. Matter 23 (2011), 325401, https://doi.org/10.1088/0953-8984/23/32/325401.
[29] X. Chen, X. Liu, K. Huang, Synthesis of uniform hexagonal ag nanoprisms with controlled thickness and tunable surface plasmon bands, Int. J. Miner. Metall. Mater. 26 (2019) 796–802, https://doi.org/10.1007/s12613-019-1785-x.